10-15-2003

Magnetic Storage Device Using Induced Magnetic Reversal of a Cobalt Element Array

Hanning Chen
University of New Orleans

Scott L. Whittenburg
University of Montana - Missoula, scott.whittenburg@umontana.edu

Magnetic storage device using induced magnetic reversal of a cobalt element array

Hanning Chen and Scott L. Whittenburg[a)]
Department of Chemistry and Advanced Materials Research Institute, University of New Orleans, New Orleans, Louisiana 70148

(Received 1 April 2003; accepted 24 July 2003)

The effects of the applied field, cell size, and cutting area on the ''seed'' induced magnetic reversal of a cobalt element array have been studied by a stochastic dynamic micromagnetics code using the Laudau–Lifshitz–Gilbert equation. Three magnetic reversal mechanisms under different magnitudes of the applied field have been investigated by examining the energy profiles. To minimize the effect of the thermal fluctuations on the switching time, an applied field with magnitude around 0.7 or 0.8 T and an element array with cutting area less than 10 nm$\times$10 nm are required. By using the smaller cellsize, the switching time and the storage density of the element array can be improved. A sinusoidal applied field with a period of 0.1 ns was used to generate a single switching event. © *2003 American Institute of Physics.* [DOI: 10.1063/1.1609654]

I. INTRODUCTION

Patterned magnetic media has been studied extensively due to possible application to ultrahigh density storage.[1,2] Interest in patterned media has spurred the development of optical lithography.[3–6] When the size of the storage element decreases to several nanometers, it becomes thermally unstable or superparamagnetic. To overcome this limitation to ultrahigh density storage, a method to store information by the position of the domain wall[7–11] in an element array rather than in the magnetic domains, was proposed in our previous article.[12] A schematic diagram of the device is given in Fig. 1. The device consists of two segments: a short segment (four spins or ''pillars'') which acts as a seed and a long segment (20 pillars) in which the information is stored. Initially the spins in the seed are oriented in a fashion so as to generate a domain wall between the seed and the element array. The domain wall can be moved into any position in the element array by applying an applied field with a finite pulse width along the easy or long axis of the element array. In this manner information can be stored in the device in terms of the position of the domain wall within the element array. In this article, the spin reversal mechanisms under different magnitudes of applied field were examined to investigate the effect of thermal fluctuations on this device. The thermal effect was also examined on element arrays with different cutting area and cell size. The cutting area is the area of the device obtained by intersecting a plane perpendicular to the long axis of the device. In addition, a sinusoidal external field was applied to switch a single pillar during each period. In this manner, the number of switched pillars can be controlled using the number of magnetic field periods.

II. COMPUTATIONAL MODEL

Our model storage device consisted of two segments of the same magnetic material. The two segments have the same cutting area but different lengths. The long segment served as the element array where the information was stored. The short segment served as the ''seed'' to generate the domain wall. Both segments are modeled as a box of cubic cells with exchange constant $A=1.4\times10^{-11}$ J/m, uniaxial anisotropy $K_1=5.0\times10^5$ J/m^3, and saturation magnetization $M_s=1.4\times10^6$ A/m.[13] These magnetic parameters are suitable for simulations on cobalt. A six-neighbor scheme was used to calculate the exchange field. We assume that all of the cells have their easy axis along the long axis of the segment.

The time evolution for the magnetization moment of each cell can be obtained from integrating the Laudau–Lifshiftz–Gilbert equation

$$\frac{dM_i}{dt}=\frac{\gamma_0}{1+\alpha^2}M_i\times\left(H_i-\frac{\alpha}{M_s}M_i\times H_i\right), \tag{1}$$

where i indicates the ith cell, γ_0 the gyromagnetic ratio of 1.76×10^{11} s^{-1} T^{-1}, α the damping coefficient, which was set as 0.1 in our calculations, M_i the saturation magnetization of cell i and H_i the effective field on cell i which includes exchange, anisotropy, Zeeman, magnetostatic, and thermal field. A fast Fourier transform algorithm was applied to accelerate the evaluation of the computationally expensive magnetostatic term.[14] According to the fluctuation–dissipation theorem,[15,16] the thermal effect can be modeled by a stochastic field $H_i(t_i)$ which fluctuates independently for each spin. This random field has a zero mean and a Gaussian distribution for the second moment given by

$$\langle H_i(t_i)\rangle=0,$$

$$\langle H_i(t_i)H_j(t_j)\rangle=\frac{2\alpha k_bT}{\mu_0M_sV}\delta(t_i-t_j)\delta_{ij}, \tag{2}$$

where k_b is the Boltzmann constant, 1.38×10^{-23} J/K, μ_0 is the magnetic permeability of free space 1.26×10^{-6} N/A^2, T is the temperature, V is the cell volume, $\delta(t_i-t_j)$ is the

a)Author to whom correspondence should be addressed; electronic mail: swhitten@uno.edu

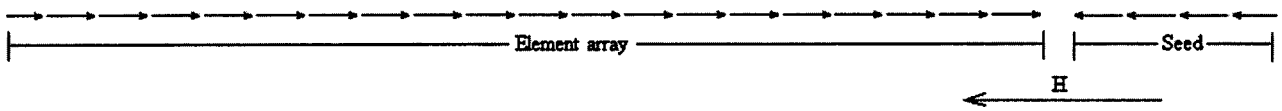

FIG. 1. A schematic diagram of the device.

Dirac delta function, and δ_{ij} is the Kronecker delta. All of the calculations in this article were done at 300 K.

Initially, all of the spins in both the element array and seed remained aligned along the easy axis direction even in the absence of an external field applied. This is due to the strong anisotropy interactions in bulk cobalt. Cobalt is a magnetically hard material. A domain wall was generated by reversing the spins in the seed segment. An external field was applied along the easy axis for a finite duration to reverse a specific number of spins in the element array and pin the domain wall in a specific position.

III. RESULTS AND DISCUSSION

An external magnetic field was applied along the easy axis of an element array with cellsize 2.5 nm and dimension 50 nm$\times$5 nm$\times$5 nm (20 cell$\times$2 cell$\times$2 cell). Field amplitudes less than 0.25 T were not able to overcome the energy barrier needed to propagate the domain wall. For field amplitudes greater than 1.50 T, magnetic reversal occurred randomly both spatially and temporally in the element array and the spins did not switch consecutively along the easy axis. In the field amplitude range between 0.25 and 1.50 T, a domain wall was observed to propagate along the easy axis. Since the spins in the plane perpendicular to the easy axis rotated coherently due to the strong exchange interaction, the array can be divided into ''pillars'' each pillar consisting of all of the spins in the same plane. We traced the reversal of the pillars in the element array and recorded the first-passage time of each pillar. The first-passage time is the time at which the pillar crosses the plane perpendicular to the easy axis. Since flipping of the spins after reversal was improbable due to the combined effect of anisotropy and external field interactions, the fist-passage time was also the switching time. One hundred simulation runs were performed for each of four applied fields and a statistics analysis carried out (Fig. 2). The propagation of the domain wall depended on the magnitude of the applied field. The reversal time for the entire element array can vary from 1.40 ns for the lowest field, 0.50 T, to 0.50 ns for the highest field, 1.10 T. The effect of thermal fluctuations on the switching time is indicated by the error bars in Fig. 2. Thermal noise manifests itself as a variance in the switching time of an individual pillar. This variance gives rise to the error bars in Fig. 2. We can define a signal-to-noise ratio (SNR), as the ratio of the average height of the error bars to the average switching times between the neighboring pillars. With the definition of SNR, the information stored in the element array is thermally stable and easily determined so long as the SNR is greater than 2. We have determined the SNR at eleven fields with magnitudes from 0.3 to 1.3 T (Fig. 3). The thermal fluctuation had minimum effect at applied field magnitudes of 0.7 and 0.8 T. At larger or smaller fields the SNR decreases. Thus, only fields with magnitudes from 0.6 to 1.0 T have an SNR$>$2 and are practical in this device application.

Because the SNR is an indication of the effect of the thermal fluctuations on the local magnetic field, the different SNRs suggest different magnetic reversal mechanisms. To study the magnetic reversal mechanism, we scanned the energy of a spin and the angle θ between the spin and the easy axis as a function of time at three different fields, 0.4, 0.7, and 1.4 T (Fig. 4). The spin monitored was chosen to be the 10th pillar of the 20-pillar element array. In Fig. 4 the symbol ● indicates the switching time of the pillars. Labels *A*, *B*, *C*, *D*, and *E* denote the pillars prior to the pillar being monitored. Figure 4 indicates that the energy and angle of the spin are significantly altered within only three pillars of the switching pillar. From this, we can estimate the half ef-

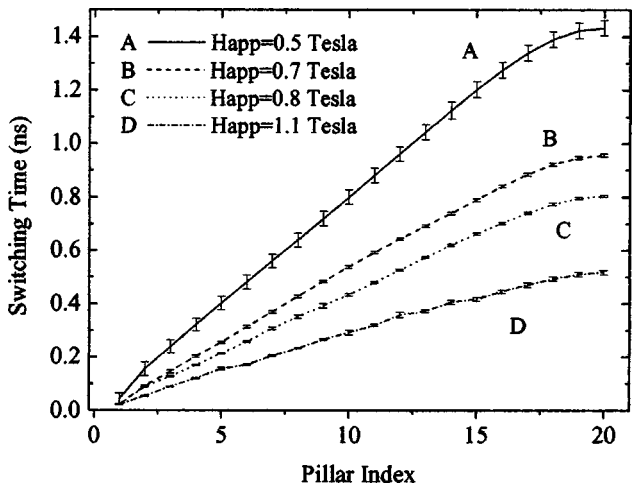

FIG. 2. Propagation of the domain wall at different applied field magnitudes.

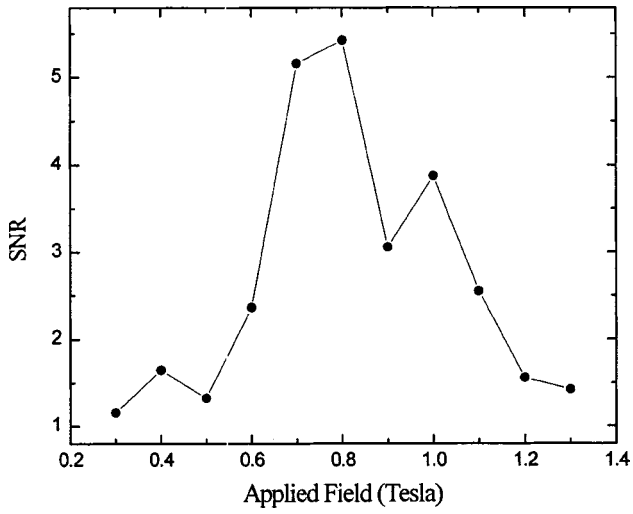

FIG. 3. SNR as a function of applied field magnitude.

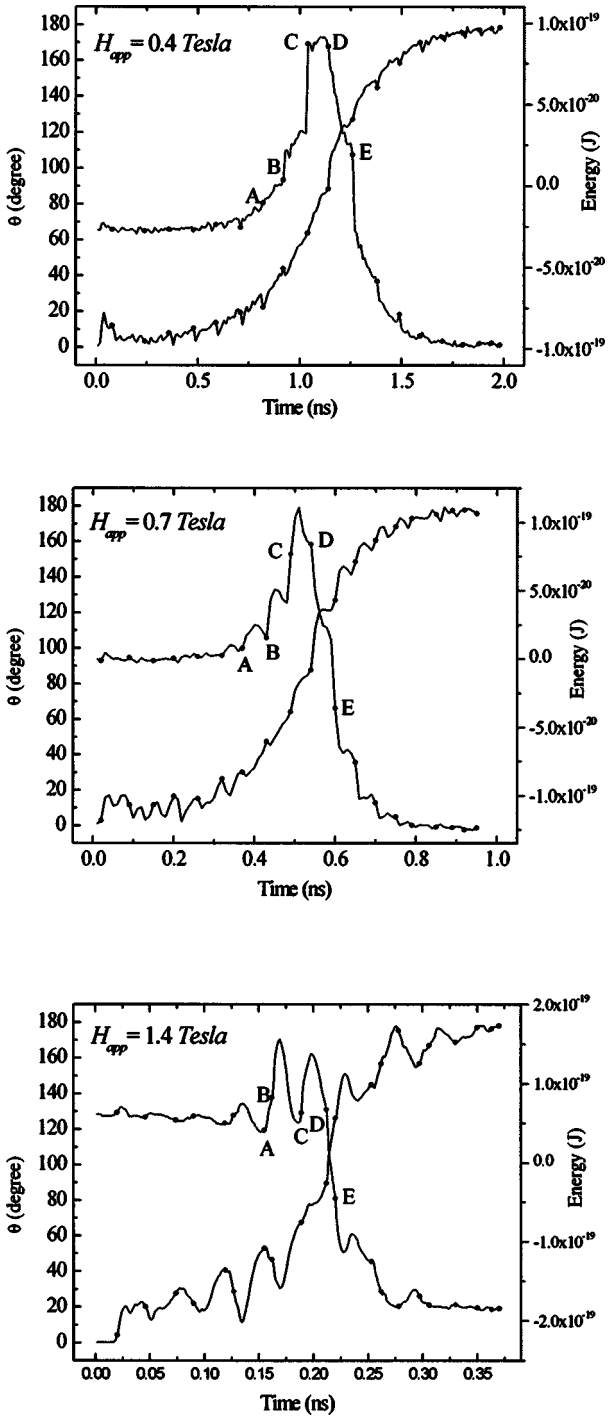

FIG. 4. Energy and θ profile with different applied field magnitudes.

fect length of the propagating domain wall to be 7.5 nm (three cells). With this information, we seek to understand why the SNR decreases at low and high applied fields.

If the magnitude of the applied field is low [Fig. 4(a)], the energy increases as the spin rotates from one orientation or spin state to the next. This increase is mainly due to the exchange interactions as can be seen in Fig. 5. The exchange interaction does not have a preferred orientation relative to the pillar array. Therefore, since the thermal fluctuation field is orientationally random, its effect may be to accelerate or retard the propagation of the domain wall. Thus, the variance

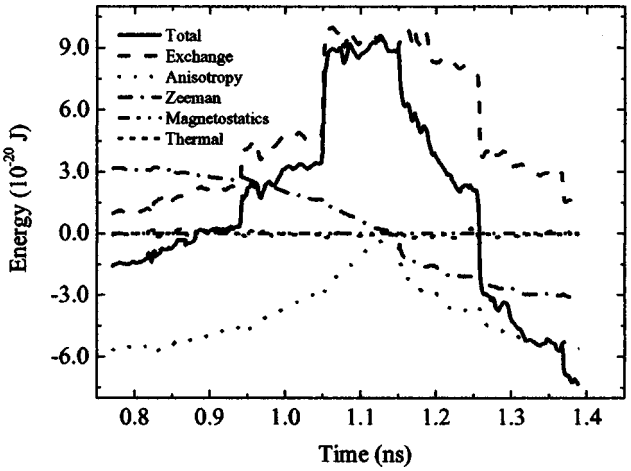

FIG. 5. High resolution energy profile at H_{app} = 0.4 T.

in the switching time and, therefore, the SNR is decreased at low applied field.

When an intermediate field is applied [Fig. 4(b)], there are two metastable points on the energy profile as the spin rotates from state *A* to state *B* or state *B* to state *C*. As the domain wall propagates, the spins in each pillar climb up the energy barrier driven by the applied field, they relax into a metastable state, and then climb up the next energy barrier. This process continues until the spin switches. At intermediate field strengths, metastable states exist in the propagating domain wall. The height of the energy barrier is large compared to the thermal field. Thus, the thermal noise is negligible at intermediate fields and a good linear relationship between the switching time and the pillar index is found as shown in Fig. 2.

At large applied fields [Fig. 4(c)], spins not adjacent to the domain wall begin to sample orientations with relatively large deviation relative to the easy axis direction. When the sum of the applied field and the thermal fluctuation field exceeds the anisotropy field for pillars adjacent to the domain wall, then the adjacent pillars also flip. This gives rise to decreased SNR at high applied fields.

Next, we examined the effect of the cutting area. From Eq. (2), we see that the thermal fluctuation can be reduced by increasing the cell volume V Since the spins within a pillar rotate coherently, it seems possible to reduce the thermal effect by increasing the cutting area of the element array. Before studying the effect of the cutting area on the domain wall propagation, we examined the coherence of the switching of the spins. Defining T_1 as the switching time difference between the switch of the first and last spins within a pillar, and T_2 as the switching time difference between the last switched spin and the first switched spin in adjacent pillar, the incoherence of the rotation can be indicated by the incoherence coefficient, $\Sigma_i^n T_{i1}/\Sigma_i^n T_{i2}$, where T_{i1} and T_{i2} are the T_1 and T_2 at pillar i respectively, and n is the number of pillars. The incoherence coefficient for different cutting areas under applied field 0.7 T is shown in Fig. 6. When the cutting area was increased, the effect of the exchange interactions between the spins in the same pillar became weaker. A large exchange interaction is needed for coherent rotation. Thus,

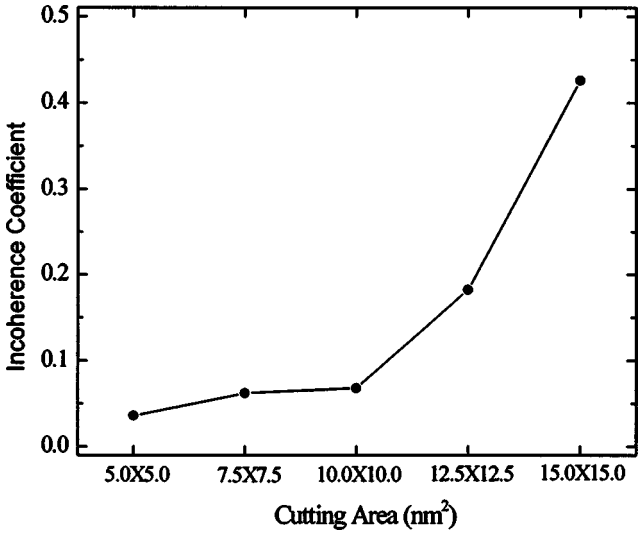

FIG. 6. Domain wall propagation with different cutting area.

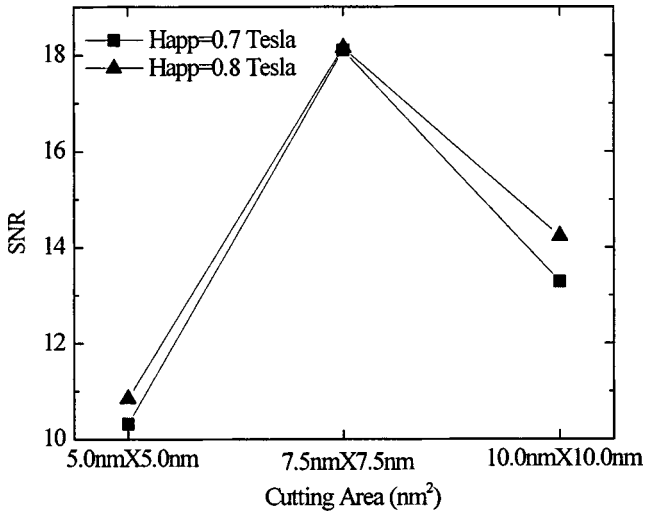

FIG. 8. SNR as a function of cutting area.

the incoherence coefficient increased with increasing cutting area as shown in Fig. 7. The incoherence coefficient increased dramatically when the cutting area was above 10.0 nm×10.0 nm (4 cells×4 cells), and the assumption of the coherent rotation was strictly valid only when the cutting area was less than 10.0 nm×10.0 nm (4 cells×4 cells).

The switching time with the indicated variance is shown in Fig. 8. For several cutting areas, 5.0 nm×5.0 nm (2 cells×2 cells), 7.5 nm×7.5 nm (3 cells×3 cells), and 10.0 nm×10.0 nm (4 cells×4 cells), the cutting area does not have a significant effect on the speed of the domain wall propagation. This is due to the strong exchange interaction between the spins within a pillar. The minimum variance was obtained at a cutting area of 7.5 nm×7.5 nm (3 cells ×3 cells) because this size was sufficiently large to overcome thermal fluctuations while maintaining coherent rotation within each pillar.

Finally, the storage density can be increased and the operating time for the device decreased if a smaller pillar is used, we tried an element array with cellsize 1.25 nm and dimension 30.0 nm×5.0 nm×5.0 nm (24 cells×4 cells ×4 cells) under applied fields of 0.7 and 0.8 T (Fig. 9). The 16 middle pillars were used to store information. Since the thermal error bars do not overlap each other, a cell size of 1.25 nm can be used. With a cell size of 1.25 nm, an areal storage density of 2×10^4 Gbit/cm^2 and an operation time to write 4 bits of information of 0.5 ns can be obtained.

In some cases, it may be easier to manipulate the information storage device if the magnetic reversal of the pillars can be controlled by "digital" signals. We simulated digital signals by a sinusoidal applied field with a period of 0.1 ns and peak magnitude 0.667 T as given by

$$H_{\mathrm{app}} = 0.667\left|\sin\left(\frac{\pi}{0.1\ \mathrm{ns}}t\right)\right|.$$

One period of such an applied field is a reasonable approximation to a field pulse. The sinusoidal field was applied to an element array with cell size 2.50 nm and dimension 50 nm ×5 nm×5 nm (20 cell×2 cell×2 cell). The switching times of the pillars were traced and indicated by ● in Fig. 10. Except for the first and last few pillars, the switching

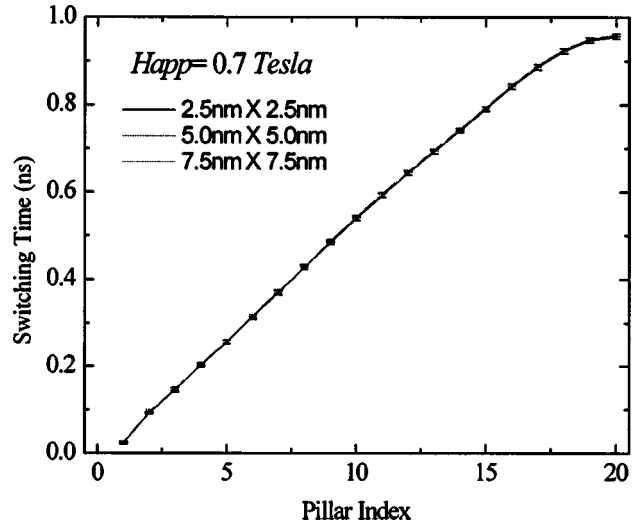

FIG. 7. Rotation incoherence coefficient with different cutting area.

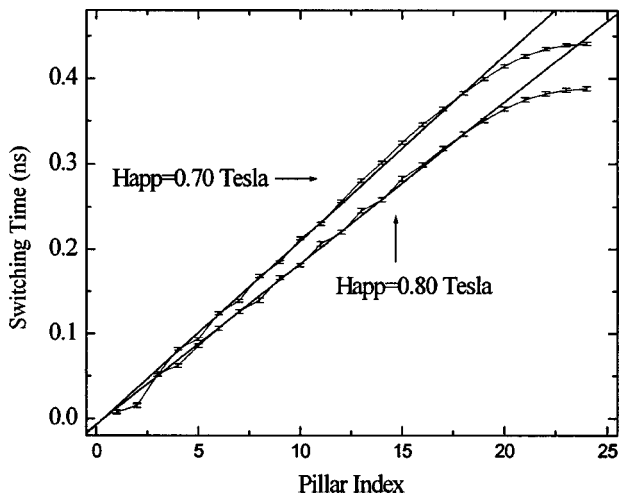

FIG. 9. Domain wall propagation with cellsize 1.25 nm.

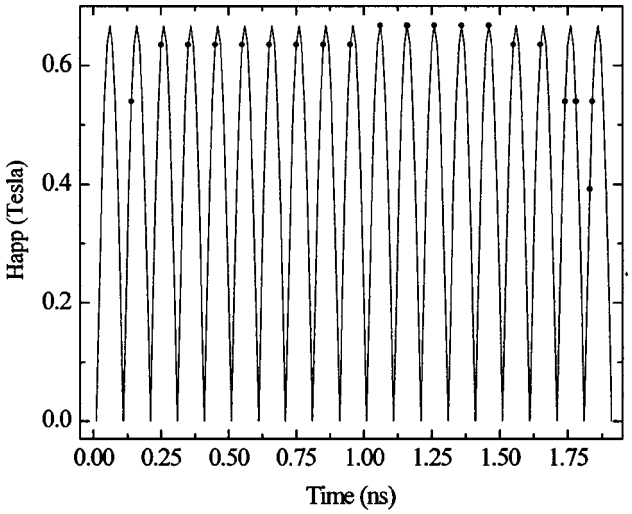

FIG. 10. Domain wall propagation under sinusoidal applied field.

event occurred when the applied field was at its peak and only one pillar switched within each period. This means that a specific number of pillars can be switched as determined by the number of applied periods of the sinusoidal field.

IV. CONCLUSIONS

The effects of the magnitude of applied field, cutting area, and cell size of the element array on the ''seed'' induced domain wall propagation have been studied. Three different magnetic reversal mechanisms under different applied fields have been investigated. To minimize the effect of thermal noise, external fields with a magnitude of 0.7 or 0.8 T and cutting areas less than 10.0 nm$\times$10.0 nm should be used. In such a device, an areal storage density of 2×10^4 Gbit/cm^2 and operation time for 4 bits of information of 0.5 ns can be obtained using a cellsize of 1.25 nm. A sinusoidal field can also be used to switch a single pillar during each period of the applied field. Our study indicates that the method of ''seed'' induced magnetic reversal can be used to store information that is thermally stable. This stability can be optimized in terms of the external magnetic field and geometry of the element array. Such devices may be viable as a fast, ultrahigh density storage medium.

ACKNOWLEDGMENTS

This work was supported by the Advanced Materials Research Institute through the Louisiana Board of Regent under Contract No. NSF/LEQSF(2001-04)-RII-03. The authors thank Professor Linxiong Li, Dr. Patrick Nichols, Dr. Nguyen Dao, and Zhidong Zhao for useful discussions.

[1] M. Haast, J. Schuurhuis, L. Abelmann, J. Lodder, and T. Popma, IEEE Trans. Magn. **34**, 1006 (1998).
[2] M. Haast, I. Heskamp, L. Abelmann, J. Lodder, and T. Popma, J. Magn. Magn. Mater. **193**, 511 (1999).
[3] E. Girgis, J. Schelten, J. Shi, J. Janeski, S. Tehrani, and H. Goronkin, Appl. Phys. Lett. **76**, 3780 (2000).
[4] L. Torres, L. Lopez-Diaz, O. Alejos, and J. Iniguez, Physica B **275**, 59 (2000).
[5] R. P. Cowburn, J. Phys. D **33**, R1 (2000).
[6] M. Herrmann, S. McVitie, and J. N. Chapman, J. Appl. Phys. **87**, 2994 (2000).
[7] A. O. Adeyeye and M. E. Welland, J. Appl. Phys. **92**, 3896 (2002).
[8] H. Forster, T. Schrefl, D. Suess, W. Scholz, V. Tsiantos, R. Dittrich, and J. Fidler, J. Appl. Phys. **91**, 6914 (2002).
[9] V. V. Osipov, E. V. Ponizovskaya, and N. García, Appl. Phys. Lett. **79**, 2222 (2001).
[10] R. P. Cowburn, D. A. Allwood, G. Xiong, and M. D. Cooke, J. Appl. Phys. **91**, 6949 (2002).
[11] A. Zhukov, Appl. Phys. Lett. **78**, 3106 (2001).
[12] H. Chen and S. Whittenburg, Science (submitted).
[13] G. Bertotti, *Hysteresis in Magnetism: for Physicists, Materials Scientists, and Engineers* (Academic, San Diego, CA, 1998).
[14] N. Hayashi, K. Saito, and Y. Nakatani, Jpn. J. Appl. Phys., Part 1 **35**, 6065 (1996).
[15] W. F. Brown, Jr., Phys. Rev. **130**, 677 (1963).
[16] W. F. Brown, Jr., IEEE Trans. Magn. **15**, 1196 (1979).